Available online at www.sciencedirect.com
SCIENCE DIRECT
Polymer 46 (2005) 11340–11350
polymer
www.elsevier.com/locate/polymer

Chain conformational transformations in syndiotactic polypropylene/layered silicate nanocomposites during mechanical elongation and thermal treatment

Vasilis G. Gregoriou *, Georgia Kandilioti, Stavros T. Bollas

Foundation for Research and Technology-Hellas, Institute of Chemical Engineering and High Temperature Chemical Processes (FORTH/ICE-HT), P.O. Box 1414, Stadiou St, 26504 Patras, Greece

Received 8 February 2005; received in revised form 27 July 2005; accepted 4 October 2005
Available online 27 October 2005

Abstract

Polymer nanocomposites prepared by melt-mixing syndiotactic polypropylene (sPP) with a quaternary modified montmorillonite have been studied with FT-IR and XRD spectroscopic techniques. FT-IR spectroscopic analysis has shown that the addition of the nanoclay results in a higher helical content for the syndiotactic polypropylene matrix. Furthermore, FT-IR spectroscopy showed that the presence of the nanoclay hinders the polymeric chains from achieving the degree of transformation from helical to *trans*-planar form during the application of mechanical stress compared to the neat sPP case. Accordingly, the sPP nanocomposites show a higher tendency relative to neat sPP to return to the initial helical conformation upon either releasing the applied mechanical tension or upon exposing to heat at 120 °C. Additionally, XRD patterns provided evidence that the use of low concentration of nanoclay (1%) resulted in partially exfoliated nanocomposites, while only intercalated nanostructures were produced at high nanoclay contents (10%). However, the application of stress can improve the degree of exfoliation of an sPP nanocomposite. In addition, linear dichroic infrared measurements which allow the monitoring of the influence of the nanoclay on the orientation of the polymeric chains during the application of stress showed that the *trans*-planar infrared bands exhibit lower orientation in comparison to the same bands in neat sPP, while the addition of nanoclay has no particular influence on the orientation of the infrared bands that are related to helical conformations. Finally, dynamic mechanical analysis (DMA) verified the enhanced mechanical properties of the sPP nanocomposites relative to neat sPP, whereas differential scanning calorimetry (DSC) depicted a slight increase in the glass transition temperature of the polymeric matrix in these nanocomposites, especially for low clay concentrations.

Keywords: Nanocomposites; FT-IR; Conformational transformations

1. Introduction

Organic–inorganic nanometer composites and especially those systems that are based on organic polymers and inorganic clay minerals consisting of layered silicates have attracted the interest of many studies in recent years after the initial reports from the Toyota research group [1–3]. The polymer nanocomposites were found to exhibit enhanced properties synergistically originated from both of the two components of the composite materials. In particular, reports on enhanced mechanical properties [3–6], thermal stability [7], fire retardant properties [8,9], biodegradation [10], gas barrier properties and ionic conductivity [11] can be found in the literature. Two types of structures of polymer/layered silicate nanocomposites can be obtained depending on the degree of dispersion of the nanoclay in the polymeric matrix: intercalated structures or exfoliated structures [12,13]. In the case of poor dispersion, the structure obtained is a conventional phase separated composite (microcomposite). In the intercalated structure the polymer chains are intercalated between the silicate layers increasing in this way their gallery height but maintaining their layered stacking resulting in a well ordered multilayer with alternating polymer/silicated layers. On the other hand, in the exfoliated structure the silicate layers lose their stacking and are exfoliated and dispersed in the continuous polymeric matrix.

Three different experimental procedures have been reported so far to fabricate the polymer/layered silicate nanocomposites: (a) the solution-intercalation method in which a polymer or a prepolymer is dissolved in a solution with the clay [14], (b) the in situ polymerization method, where a monomer is dissolved in a solution with the clay followed by in situ polymerization [15], and (c) the direct melt intercalation method in which

* Corresponding author. Tel.: +30 2610 965205; fax: +30 2610 965223.
E-mail address: gregoriou@iceht.forth.gr (V.G. Gregoriou).

0032-3861/$ - see front matter © 2005 Elsevier Ltd. All rights reserved.
doi:10.1016/j.polymer.2005.10.026

the polymer is melt-mixed with the clay above the softening point of the polymer [16]. Melt-intercalation is a very prominent procedure since the use of organic solvents is not required and could be easily applied in industry. A crucial factor for succeeding exfoliated structures is the organic modification of the silicate layers so that they can be miscible or compatible with the hydrophobic polymeric matrix. Cationic exchange between the silicate layers with long chain alkylammonioum cations reduces their surface hydrophilicity favoring the interaction with the polymeric chains.

Several polymer nanocomposites based on polyethylene [17], polypropylene [3,18], polyamide-6 [19], polylactide [20] etc have been prepared using the melt-intercalation method. The use of polyolefins as a polymeric matrix is preferable due to their wide use in the industry and their low cost. Contrary to the abundance of studies on isotactic polypropylene nanocomposites, the formation and investigation of nanocomposites based on syndiotactic polypropylene only very recently has been reported for the first time [21]. Neat sPP has gained great scientific interest in recent years, primarily due to the development of new metallocene catalysts that allow the synthesis of polyolefins of stereoregularity, purity and yield [22]. The necessity to improve the less efficient properties of sPP (considerably lower crystallinity, maximum achievable tensile modulus and strength) in comparison to iPP, as well as the very complicated polymorphism of this polymer combined with the lack of studies on sPP layered silicate nanocomposites makes this area of polymer research very attractive.

When the crystalline structure of sPP is considered, the existence of four crystal forms of sPP has been confirmed so far. The first crystalline form, depicted as form I, is the most stable form obtained under the most common conditions [23,24]. It consists of repeated *trans–trans–gauche–gauche* molecular sequences, $(T_2G_2)_n$ and is characterized by chains in helical conformation [23,25,26]. In this form the helical chains are antichiral [23,24] with an alternation of right-handed and left-handed helices along both axes of an orthorhombic [23] unit cell with axes $\alpha=14.5$ Å, $b=11.2$ Å and $c=7.4$ Å. A refinement of the crystal structure of form I has been proposed by De Rosa et al. [27], which has a unit cell of a lower symmetry with axes $\alpha=14.31\pm0.07$ Å, $b=11.15\pm0.02$ Å, $c=7.5\pm0.1$ Å and $\gamma=90.3\pm1.5°$. In contrast, form II, corresponds to a C-centered structure [26] which consists also of helical chains and the helices have the same chilarity [26,28]. Chains in form II are packed in an orthorhombic unit cell with axes $\alpha=14.5$ Å, $b=5.6$ Å and $c=7.4$ Å [27]. This form can be obtained by annealing fiber samples of sPP [25,26] or by stretching compression molded sPP samples with low stereoregularity [26,28]. Form III is a metastable form of sPP which can be obtained through cold drawing of samples quenched from melt at low temperatures [29] or by stretching compression molded sPP samples with high stereoregularity at room temperature [25,28,30]. This form is characterized by chains in *trans*-planar conformation [31] which are packed in an orthorhombic unit cell with axes $\alpha=5.22$ Å, $b=11.17$ Å and $c=5.06$ Å [29]. The *trans*-planar form III can be spontaneously induced during quenching and holding sPP samples into ice–water for several hours [32–35]. In this case, although the chains adopt the *trans*-planar conformation this form cannot be identified as the known crystalline form III, but rather as a mesophase, or also paracrystalline, disordered phase [35]. Syndiotactic polypropylene of all-*trans* form (form III) is transformed to form IV characterized by chains in $(T_6G_2T_2G_2)_n$ conformation upon exposure to organic solvents vapors [36]. A triclinic structural model for this form was proposed by Chatani et al. [36] which corresponds to the packing of one chain per cell with constants $\alpha=5.72$ Å, $b=7.64$ Å, $c=11.60$ Å, $a=73.1°$, $\beta=88.8°$, $\gamma=112.0°$, space group $P1$ descriptive of local situation of order. In contrast, Auriemma et al. [37] proposed a monoclinic structural model in which two chains are included in the cell with constants $\alpha=14.17$ Å, $b=5.72$ Å, $c=11.6$ Å and $\beta=108.8°$, space group C2, descriptive of the order in the long range.

Furthermore, the main interest of several authors is focused on the crystalline phase transformations that take place between the various forms of sPP upon exposure to stress or heat. For instance, stretching an sPP sample of form I, the chains that initially adopt the helical conformation transform into a configuration where the *trans*-planar conformation dominates. Additionally, some authors believed that upon releasing the applied stress of sPP samples in form III the pure form II can be obtained [28,38,39]. On the other hand, Guadagno et al. [40,41] believe that the released samples transform towards different forms with a memory of the initial structure. In particular, they showed evidence that the samples transform into oriented helical structures if the structure before the tension was form I type or into an oriented mesophase if the initial structure was the mesophase. In a more recent study the same authors showed that when the highly stretched sample in the crystalline *trans*-planar form III was relaxed it transformed into a less oriented mesophase, still exhibiting chains in the *trans*-planar conformation [42]. Some helical segments were also formed but they reside in the amorphous domains. Our recent publication [43] is more in agreement with the last mentioned studies since we have found that when the samples are released from the tension the reversal to the initial helical structure is not complete but the macromolecular chains result in a mixture of helical and *trans*-planar conformations.

In addition, many authors have extensively studied the effect of heat on the various polymorphs of sPP which also induces phase transformations. However, there is also contradiction among these studies. For instance, in the case of the thermal treatment of the *trans*-planar conformation, there is disagreement about the temperature region where the phase transformation takes place and the exact structure in which the *trans*-planar form is transformed. Bonnet et al. [44] mentioned that when a highly stretched sPP sample in the *trans*-planar form III is annealed, a retransformation of the *trans*-planar chains into the helical chain conformation is achieved above 80 °C. On the other hand, some studies mentioned that this retransformation is achieved above 100 °C [29] and the result is a mixture of crystals of forms I and II [28]. Yet, other authors [45,46] using high-resolution solid-state ^{13}C NMR spectroscopy reported that the

transformation takes place at about 50 °C. However, there is also disagreement about the role of the *trans*-planar mesophase on the behavior of the annealed samples. Ohira et al. [47] believe that for samples crystallized at 0 °C (*trans*-planar mesophase) the temperature for the crystal transformation from form III to II is about 40 °C, while the transformation from form III to form I takes place at about 60 °C. Vittoria et al. [35] mentioned that the *trans*-planar mesophase is stable up to 80 °C, whereas at 90 °C these authors found that it is almost completely transformed into the more stable form I. Still, in a more recent study [48] it was observed by X-ray and FT-IR spectroscopic techniques that annealing released samples (*trans*-planar mesophase) the mesophase is transformed into forms I and II between 60 and 80 °C, both of them highly oriented, while upon annealing the samples at constant strain in which the *trans*-planar mesophase was not present, no formation of the helical form II was observed and only a mixture of the *trans*-planar form III and the helical form I developed. Finally, there is also disagreement if the samples should be kept under constant strain or not during the annealing in order to succeed the transformation from *trans*-planar to the helical conformation. Loos et al. [49] reported that the transformation cannot be succeeded by annealing at 60 °C when the sample was kept strained during annealing, while other studies [25] mentioned that during the annealing of compression-molded samples with *trans*-planar conformations obtained by drawing at room temperature the ends of the samples should be kept fixed in order to obtain the transition to the helical conformation.

Infrared spectroscopy is a powerful and well-known technique which has been used extensively in polymer characterization studies by providing information on chemical nature, conformational order and molecular orientation [50]. FT-IR was used in this study in order to monitor the phase transformations of the polymeric matrix in sPP nanocomposites upon mechanical and thermal treatments relative to the presence of the nanofiller in the polymeric matrix. In addition, XRD spectroscopy was employed in order to investigate the intercalation of the nanocomposites and the effect of the stress on the intercalation. Finally, DMA and DSC measurements were used to explore the mechanical and thermal properties of the nanocmposites.

2. Experimental section

2.1. Materials

Cloisite 20A, a natural montmorillonite modified with a quaternary ammonium salt with cation exchange capacity of 95 mequiv./100 gr clay (Southern Clay, Inc, USA), was used as a nanofiller in the preparation of the nanocomposites. Sixty eight percent stereoregular syndiotactic polypropylene (sPP) in droplets was used as a polymeric matrix. The melting temperature of sPP was about 125 °C while the M_w was 135, 000 ($M_w/M_n = 2.2$).

2.2. Composite preparation

All the nanocomposites were prepared by melt compounding in a home-made batch-mixer. Before the melt-mixing Cloisite 20A was dried in vacuum at 80 °C for at least 16 h (over night). Afterwards, the two components were premixed for 3 min and then they were melted in batch-mixer for 3 min. Finally, they were melt-mixed for 3 min at 170 °C with a speed of mixing around 60 rpm.

2.3. Film preparation

In order to prepare films of desirable dimension 1.4 g of nanocomposite were pressed with pressure of 200 bar at ~170 °C. After quenching at 0 °C for 20 min, films with dimensions $3 \times 0.65 \times 0.02$ cm^3 are obtained.

2.4. Apparatus and procedures

The infrared studies were carried out using a Nicolet 850 FT-IR spectrometer equipped with a MCT/A detector. Each measurement was the accumulation of 128 scans at 4 cm^{-1} spectral resolution. A 25 mm slide mount polarizer (Thermo Electron Corporation, USA) was used to polarize the plane of the light which is reaching the sample. A gradual elongation of the samples was performed on miniature mechanical tester apparatus at room temperature with a step of 50% elongation up to 600% elongation, while FT-IR spectra were recorded at each step. In order to perform the thermal infrared experiments a highly stretched sample, which was just released from the applied stress was placed on heat demountable cell kit for high temperature transmission infrared applications. The kit uses 32 mm diameter CaF_2 windows, while the temperature was increased gradually from 25 up to 120 °C with a heating rate of 5 °C. Finally, in order to estimate the transformation indexes and the dichroic ratios that are examined in this study the peak heights were used. The samples were tested 24 h after the quenching step.

For the X-ray diffraction measurements, a bragg-brentuno optics (Panalytical Corporation, USA) was employed including a fixed divergence slit (1/16°), a fixed diffracted antiscatter slit (1/16°), a fixed incident anti-scatter slit (1/8°) and an X Celerator RTMS (real time multiple strip) solid-state linear detector.

Dynamic mechanical analysis, (DMA), was performed in a solid-state analyzer RSA II, (Rheometrics Scientific C. USA), at 10 Hz with heating rate 3 °C/min.

Finally, differential scanning calorimetry (DSC) took place on a TA Instruments DSC Q 100 apparatus. The calibration was performed using an indium standard, while the heating rate was 10 °C/min. First, the samples with weight of 5–10 mg were heated up to 170 °C in order to erase previous thermal history. Then the samples were cooled at −50 °C and heated again up to 170 °C.

3. Results and discussion

Syndiotactic polypropylene nanocomposites with 1, 3, 5, 7 and 10 wt% of Cloisite 20A present were investigated in order to examine the influence of the addition of the nanoclay into the matrix. Fig. 1(a) presents the infrared spectra of the nanocomposites with the various contents of clay. The spectral region between 700 and 1000 cm^{-1} depicted in this figure includes some of the characteristic infrared bands of sPP (also see Ref. [43], Table 1). It is obvious that all these samples are characterized by polymeric chains mainly in the helical conformation since their spectra exhibit intense infrared bands which are related to the helical form of sPP (811, 867, 902 and 977 cm^{-1}). In addition, bands which are attributed to the *trans*-planar conformation are also present. For a quantitative investigation of the influence of the nanoclay on the polymeric matrix the behavior of the characteristic infrared bands of sPP can be monitored. A common pair of bands usually used is the one that is located at 977 and 962 cm^{-1}. These bands are attributed to helical and *trans*-planar conformations, respectively. We have called the ratio of the infrared absorptions of these bands transformation index in the past [43,51] and it can be used to observe the phase transformations that take place by various factors. Fig. 1(b) shows the change of the transformation index as a function of the clay content. It can be seen that the ratio begins to increase with the addition of the nanoclay in the polymeric matrix and continues to increase as the content of clay increases. This means that the nanoclay induces to the polymeric chains a preference to adopt higher levels of helical conformations relative to neat sPP. These results are in agreement with the conclusions of Lotz et al. [52], who supported the statement that helical conformation is preferable.

Besides the direct consequence of the nanoclay on the polymeric matrix during their intercalation, the interaction of the clay with the polymeric chains of a nanocomposite during the application of mechanical treatment constitutes a very interesting point in the study of nanocomposite structures. For this reason, neat syndiotactic polypropylenes and sPP nanocomposite samples in all previous mentioned concentrations of clay were subjected to different levels of elongations from 50 to 600% and the infrared spectra of each specimen at the respective elongations were simultaneously recorded. In order to investigate the behavior of the polymeric matrix and the conformational transformation that takes place during the application of stress the transformation index is again calculated. Fig. 2 shows the changes in the transformation index of the elongated nanocomposites with respect to the degree of strain. The transformation index for all samples begins to decrease sharply with the application of stress which is expected since it is known and already mentioned in the introduction part that when an sPP sample in the helical form I is exposed to mechanical stress, it begins to transform into the *trans*-planar conformation. Yet, it should be noticed that there are interesting variations among the samples. In particular, the transformation from the helical into the *trans*-planar conformation of the neat sPP seems to be completed at approximately 200% elongation where the transformation index has a value of approximately 0.3. On the other hand, in the case of the nanocomposites, the transformation seems to be completed earlier than in neat sPP at about 100% elongation. Additionally, the sPP nanocomposites seems not capable to achieve the high levels of *trans*-planar conformation like in the case of the pure sPP, since their transformation indexes vary at ~0.5. Thus, it can be assumed that the presence of the nanoclay in the

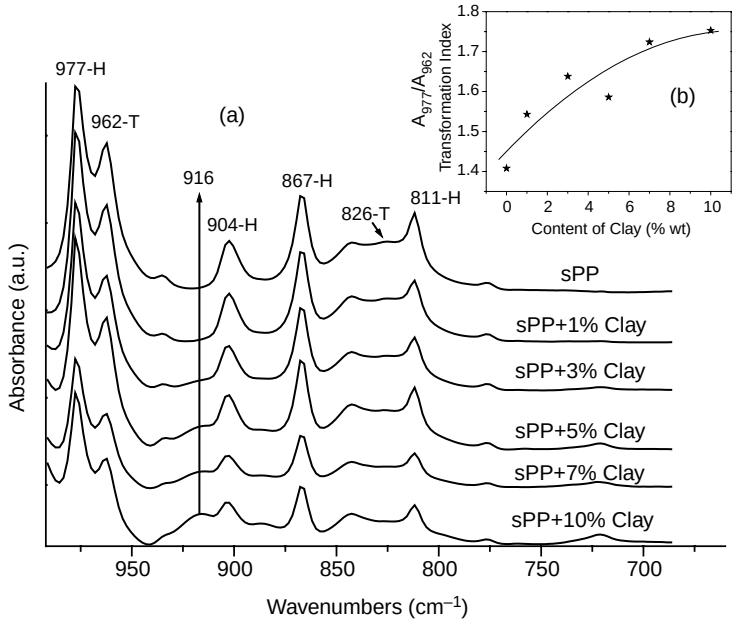

Fig. 1. (a) FT-IR spectra of sPP nanocomposites having different contents of clay (b) graphic representation of the ratio A_{977}/A_{962} ('transformation index') as a function of the content of clay.

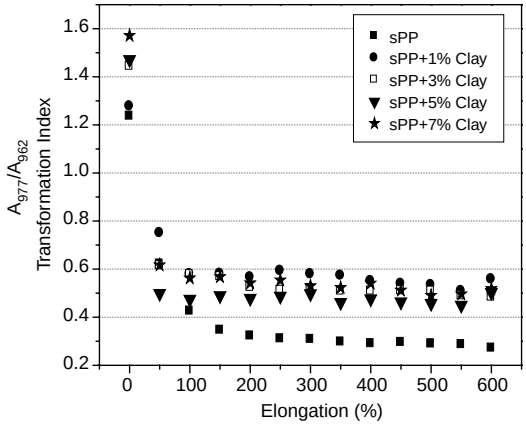

Fig. 2. Graphic representation of the ratio A_{977}/A_{962} ('transformation index') as a function of the elongation.

polymeric matrix prevents the accomplishment of a complete transformation into the *trans*-planar conformation.

Another point of this study is the investigation of the behavior of the polymeric matrix in the sPP nanocomposites after the release of the applied tension. According to a recent study by our group [43], when an sPP specimen is released from the steady tension, a transformation from the *trans*-planar conformation into a mixture of helical and *trans*-planar conformations takes place. In particular, we have found that the sPP sample do not return completely into the initial helical conformation before the application of stress. In order to monitor the phase transformations that take place during the release of tension in the sPP nanocomposites, the transformation index was again estimated and the results are depicted in Fig. 3. In this figure, it can be clearly seen that the sPP nanocomposites exhibit a different behavior from the neat sPP specimens. Although their polymeric chains also transform into a mixture of helical and *trans*-planar forms, these polymeric chains manifest a tendency to turn into higher levels of helical conformations, since their transformation indexes (0.7) are higher than that of the neat sPP (0.5). Fig. 3 shows that the phenomenon of retransformation of the polymeric chains upon relaxation is time-depended [43], since we can observe that the phase transformation during the relaxation continues to take place even after a month from the release of tension. Yet, the helical conformation levels remain higher for the sPP nanocomposites. In addition, it has been found that the elasticity of sPP is closely associated with the reversible transition from the *trans*-planar to the helical conformation [38].

In Fig. 4(a) and (b) the X-Ray diffraction patterns of the sPP nanocomposites with 1 and 10% nanoclay content in both unstretched and relaxed modes are reported. In order to investigate whether intercalation or exfoliation is taking place, the diffractogram of Cloisite 20A is also shown in which a diffraction peak is observed at $2\theta = 3.6°$. This means that that a basal spacing of 24.5 nm characterizes this particular nanoclay. In the case of the sPP nanocomposite with 1% loading of nanoclay, Fig. 4(a), the main diffraction peak is shifted at $2\theta = 2.8°$, while the other two accompanying peaks at 4.5 and 7.3° have decreased relatively to the main peak, an indication of the presence of an intercalated structure. On the other hand, in the case of the nanocomposite with 10% loading, Fig. 4(b), the peak that was used to calculate the basal spacing is shifted less ($2\theta = 3.2°$), while the other two peaks are still distinct denoting partial intercalation. Therefore, the use of lower concentrations

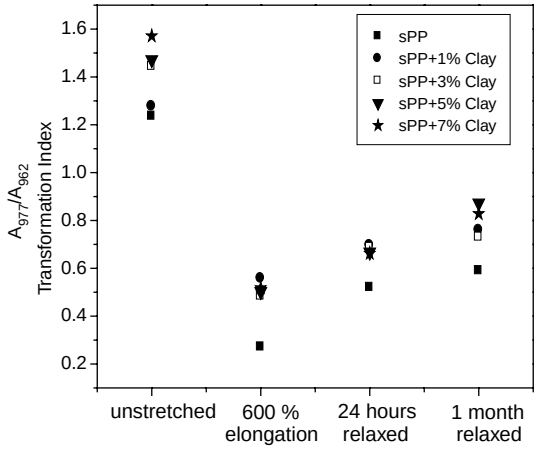

Fig. 3. Graphic representation of the ratio A_{977}/A_{962} ('transformation index') for the unstretched, 600% elongated and relaxed sPP nanocomposites with different contents of clay.

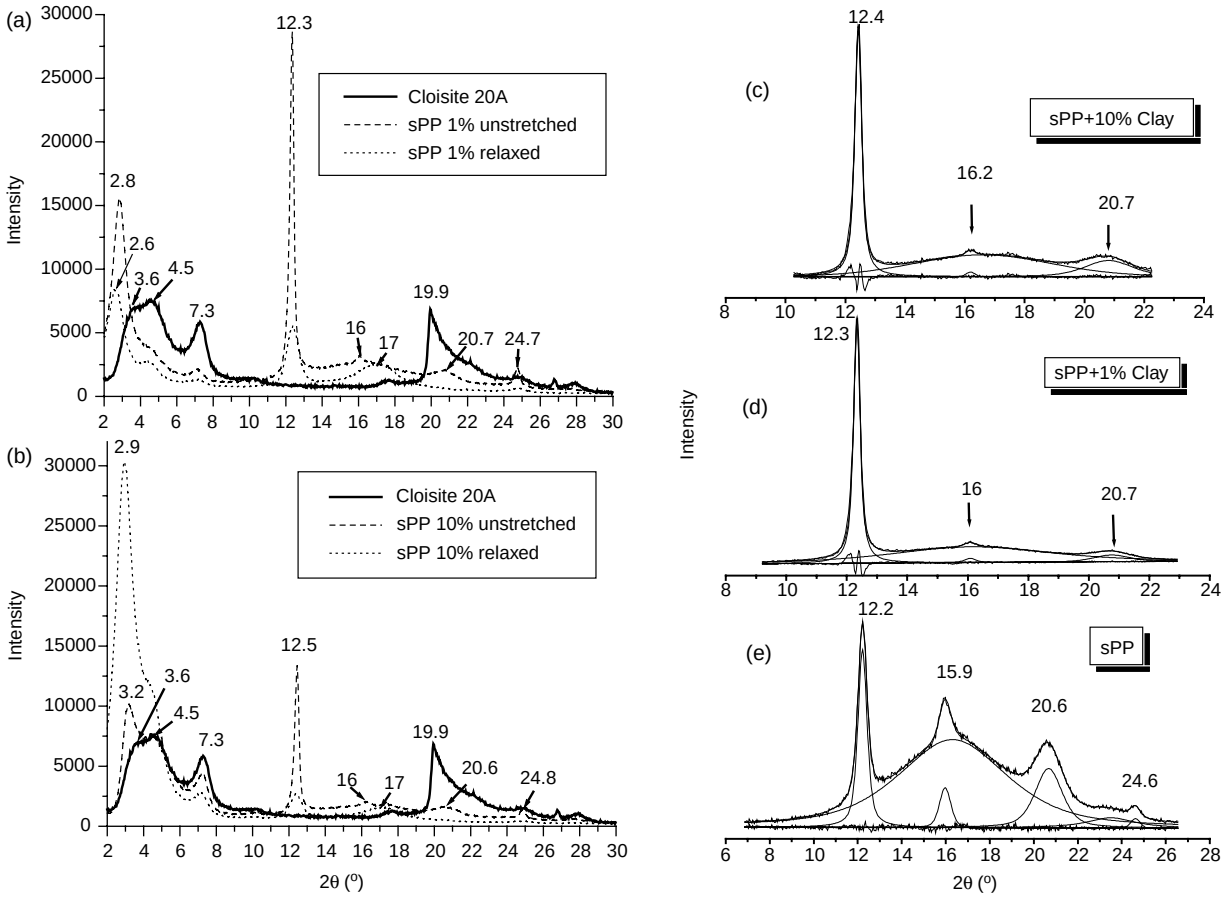

Fig. 4. Comparison of X-ray diffraction patterns for (a) pure cloisite 20A with a stretched and a relaxed specimen of sPP with 1% clay, (b) pure cloisite 20A with a stretched and a relaxed specimen of sPP with 10% clay, and deconvolution of the X-ray diffraction patterns of (c) neat sPP, (d) sPP with 1% clay and (e) sPP with 10% clay.

of nanoclay is preferred for achieving intercalated structures. Furthermore, Fig. 4(a) and (b) show that the application of stress is an additional factor which can improve the intercalation level in nanocomposites. The XRD patterns of the highly stretched and then relaxed samples show that the applied tension favors the exfoliation of the silicate layers in the polymeric matrix since the already intercalated nanocomposites with 1% nanoclay, Fig. 4(a), appear to be partially exfoliated due to the fact that the first diffraction peak is even more shifted ($2\theta = 2.6°$) and exhibits a small decrease relatively to the unstretched sample. Simultaneously, the partially intercalated nanocomposite of 10% loading, Fig. 4(b), show an increase in the level of intercalation during the application of stress since the main diffraction peak is shifted at 2.9°. Yet, it should be noted that although the peak used to calculate the basal spacing is obviously decreased when the intercalation or the exfoliation is taking place, in the case of the relaxed sPP nanocomposite with 10% clay the relative intensity of this peak is significantly increased. We believe that in this sample before the application of stress the nanoclay was not well dispersed into the polymeric matrix and as a result when the stress is applied to the sample, the polymeric matrix carries along the silicate layers and force them to orient. The concentration of the clay is high enough so that the orientation can be easily noticeable in the XRD pattern.

In addition, the X-ray diffraction patterns can provide also information about the behavior of the polymeric matrix relative to the content of the nanoclay and the application of stress. The X-ray diffraction pattern of neat sPP is compared with the sPP nanocomposites with 1 and 10% clay, Fig. 4((c)–(e)), respectively. The region from 11 to 26° was deconvoluted in order for the individual peaks in the spectrum to be clearly shown. All the nanocomposite samples contain the characteristic diffraction peaks of neat sPP but important differences can be observed which arise from the different crystalline conformations that the polymeric matrix adopts as the result of the application of stress or the addition of the silicate layers. In particular, the unstretched sPP nanocomposite samples contain peaks at 12.3, 16 and 20.7° and 24.7° of 2θ which are characteristic of the helical form I of sPP [23,25,40]. The amorphous halo that is observed in the case of the neat sPP decreases notably with the addition of clay. One possible explanation for this could be an increase in the crystallinity of the polymer. However, this decrease of the halo in reality is related to the change in the average mass absorption coefficient (MAS) due to the presence of the clay. The clay has 10 times

lower MAC than that sPP in Cu radiation (~30 vs. 3.74 cm^2/g) which is expected to affect the penetration depth into the sample and the overall intensity out of the sample. On the other hand, the effect of the clay on the order of the helical form is not very significant. The peak at 16° seems to become slightly broader for the nanocomposites, while the diffraction peak at 12.3° remains sharp and intense. According to Gorrasi et al. [53] the addition of clay increases the disorder of the crystalline form I but the phenomenon becomes substantially profound at high loads of clay (20%), much higher than the concentrations studied here. On the other hand, the XRD data for the samples that were subjected to mechanical stress and left to relax are in agreement with the infrared data. In particular, the diffraction peaks of form I are clearly decreased. In addition, a new diffraction peak located at 17° is observed. Since this new band appears to be significantly broad it cannot be attributed to the helical form II [25], but according to Vittoria et al. [35,40] can be identified as the *trans*-planar mesophase. Thus, we can assume that the polymeric chains after the relaxation have been turned into a mixture of helical and *trans*-planar conformations.

Furthermore, infrared linear dichroism analysis was used to investigate the effect of the application of stress on the orientation of the molecular chains of the polymeric matrix in the nanocomposites. In order to study the orientation of the sPP nanocomposites, the dichroic ratios of some of the characteristic infrared bands of the various conformations of sPP have been calculated. The dichroic ratio is defined as the ratio of the absorption intensity when the electric vector of the infrared radiation is parallel to the drawing direction of the polymer to the absorption intensity when the electric vector is perpendicular to the drawing direction. Fig. 5(a) and (b) depict the changes in the dichroic ratios of the bands located at 962 and 977 cm^{-1}, respectively for the sPP nanocomposite samples and the neat sPP for various elongation lengths (0–600%). The band at 962 cm^{-1} is attributed to the *trans*-planar conformation, whereas the band at 977 cm^{-1} is assigned to the helical conformers. Before the application of the stress the dichroic ratios for all the samples is unity, which means that the polymeric chains have an average random orientation. However, the dichroic ratio of the *trans*-planar band at 962 cm^{-1} band (Fig. 5(a)) after the application of stress is above unity which means that the transition moment of this band orients parallel to the drawing direction. Yet, the addition of the nanoclay affects the orientation of the transition moment of the band. In particular, the samples that contain nanoclay show lower orientation than that of neat sPP. Additionally, the orientation increases as the content of the nanofiller increases, Fig. 5(a). The changes in the dichroic ratio of the helical band at 977 cm^{-1} are shown in Fig. 5(b). This is also a parallel oriented band with respect to the drawing axis since the dichroic ratio after the application of stress is above unity. However, no particular influence from the nanoclay on the orientation of the helical band can be clearly observed except for the sample with 1% clay that seems to constrain somewhat the orientation of the helical band. The same sample shows the highest constrain to the orientation of the *trans*-planar band as well. According to our observations the nanocomposite with 1% of clay has a rather unique behavior when compared to the higher concentration samples.

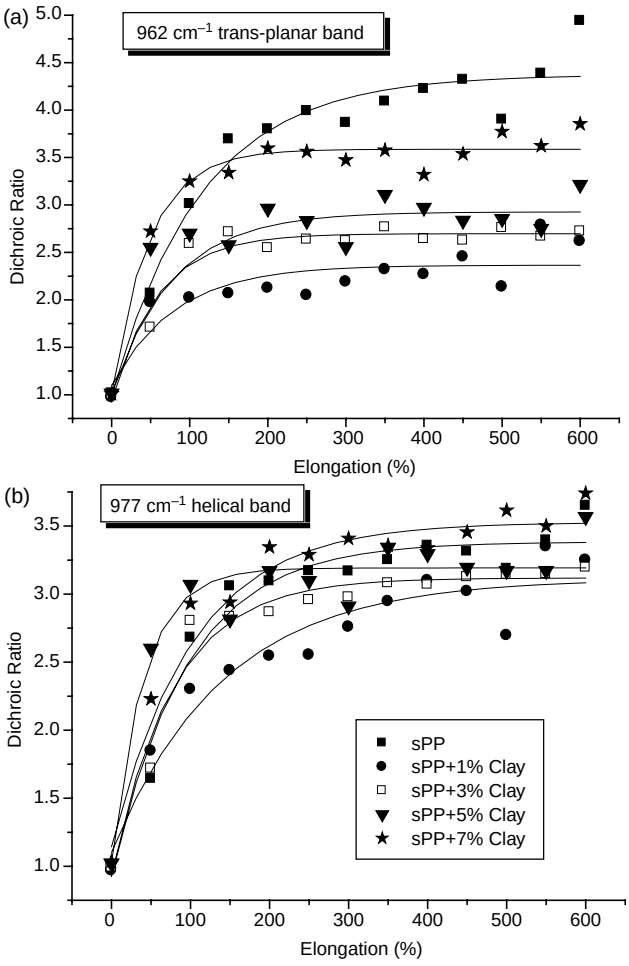

Fig. 5. Plot of the dichroic ratios for the *trans*-planar and helical infrared bands located at 962 and 977 cm^{-1}, respectively for the sPP nanocomposites with different contents of clay as a function of strain.

Furthermore, in order to investigate the influence of the presence of the nanoclay on the mechanical properties of sPP dynamic mechanical analysis (DMA) was employed. DMA allows the monitoring of the behavior of the synthesized nanocomposites under stress and temperature. Fig. 6(a)–(f) depict the dynamic mechanical properties (storage modulus E', loss modulus E'', and loss factor tan δ) for neat sPP and sPP nanocomposites as a function of the temperature as well as of the clay content. In Fig. 6(a), a slight increase in the storage modulus with the addition of clay is observed. The glass transition temperature (T_g) was estimated by taking the maximum value of the loss modulus versus temperature and was found to be 10 °C, Fig. 6(b). In addition, the values for storage, loss modulus and tan δ are shown for two different temperatures (0 and 20 °C), Fig. 6(d)–(f). These temperatures are slight above and below the range of the glass transition temperature of sPP. It can be seen that the storage and the loss modulus are increased in the case of the nanocomposites compared to the neat polymer for both temperatures. On the

other hand, Fig. 6(f), which presents the plot of tan δ as a function of the addition of clay reveals that the ratio of E''/E' (tan δ), which is proportional to the ratio of energy lost to energy stored in one cycle (loss factor) does not change with the addition of the nanoclay at 0 °C, while it shows a small decrease at 20 °C. Therefore, if high contents of clay are used above 20 °C this will result in a partial loss of the shock-proof properties of the material.

The final aspect of this study is the investigation of the behavior of the nanocomposites and mainly the conformational transformations of the polymeric matrix versus the presence of the nanoclay during thermal treatment of the samples. It is already mentioned that when a highly stretched sPP sample having its molecular chains in the *trans*-planar conformation is heated, a transformation into the helical conformation is observed. In order to monitor the phase transformations that take place during the thermal treatment the same pair of infrared bands (977, 962 cm^{-1}) is again used to calculate the ratio of the absorption of a helical band over a *trans*-planar band. Fig. 7 shows the change of this ratio during the thermal treatment for both sPP and sPP nanocomposites from room temperature up to 120 °C. At room temperature all the samples

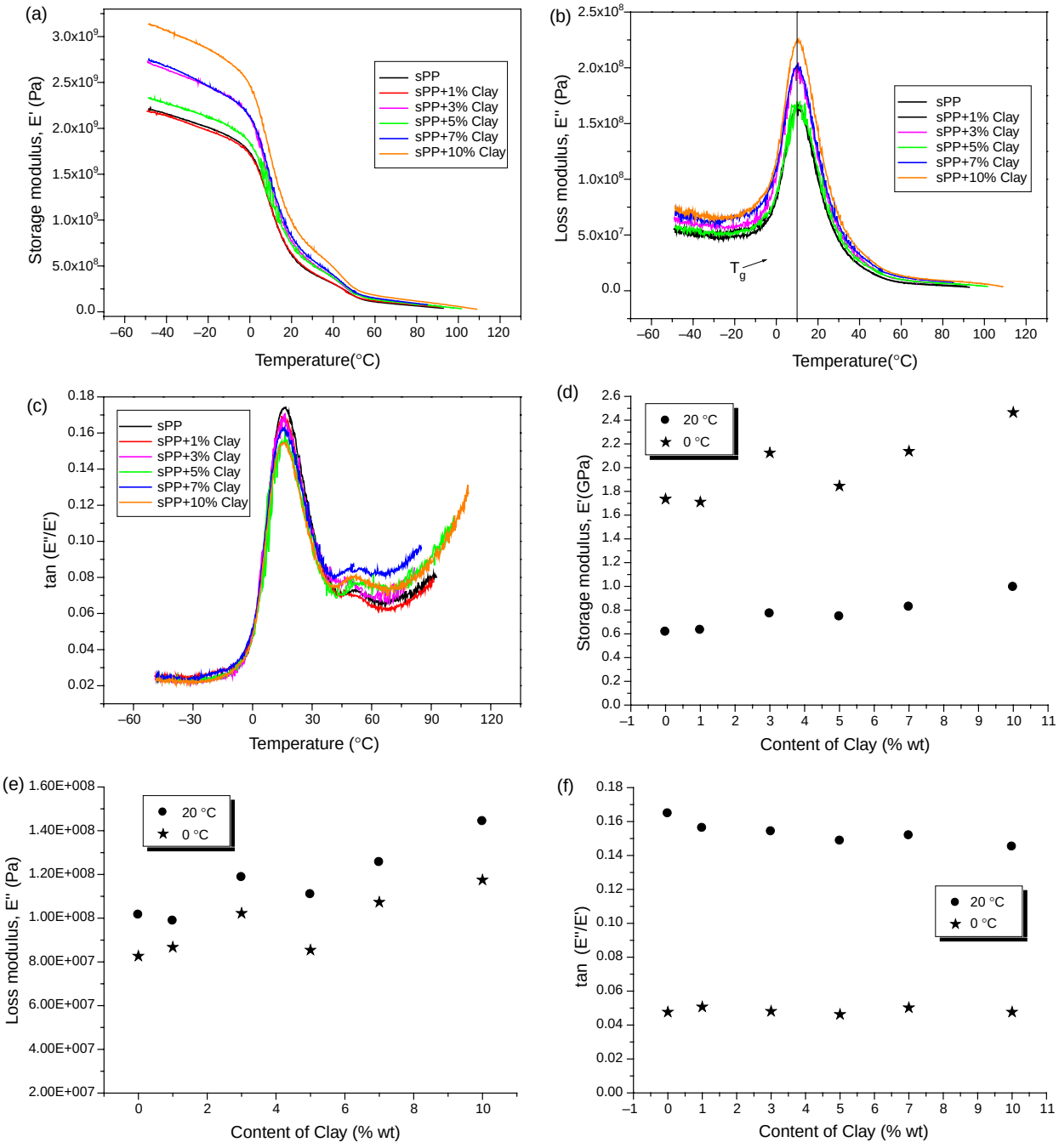

Fig. 6. Plots of (a) storage modulus E', (b) loss modulus E'', and (c) loss factor tan δ for sPP and sPP nanocomposites as a function of the temperature and plots of (d) storage modulus E', (e) loss modulus E'', and (f) loss factor tan δ f as a function of content of the nanoclay at 0 and 20 °C.

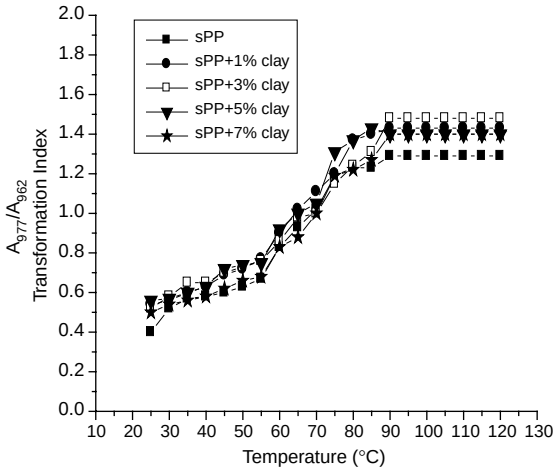

Fig. 7. Graphic representation of the absorbance ratio A_{977}/A_{962} ('transformation index') as a function of temperature for sPP nanocompomposites just released from stress.

consist of polymeric chains that are characterized mainly by *trans*-planar conformation and low contents of helical segments. However, the samples that contain the nanofiller exhibit a slight higher value of the ratio of the absorption of the helical to the absorption of the *trans*-planar band (varying between 0.54 and 0.58), which indicates again that the sPP nanocomposites contain higher proportion of helical segments respective to the neat sPP (0.52). When the temperature begins to increase, the transformation index also increases suggesting a transformation from the *trans*-planar conformation into

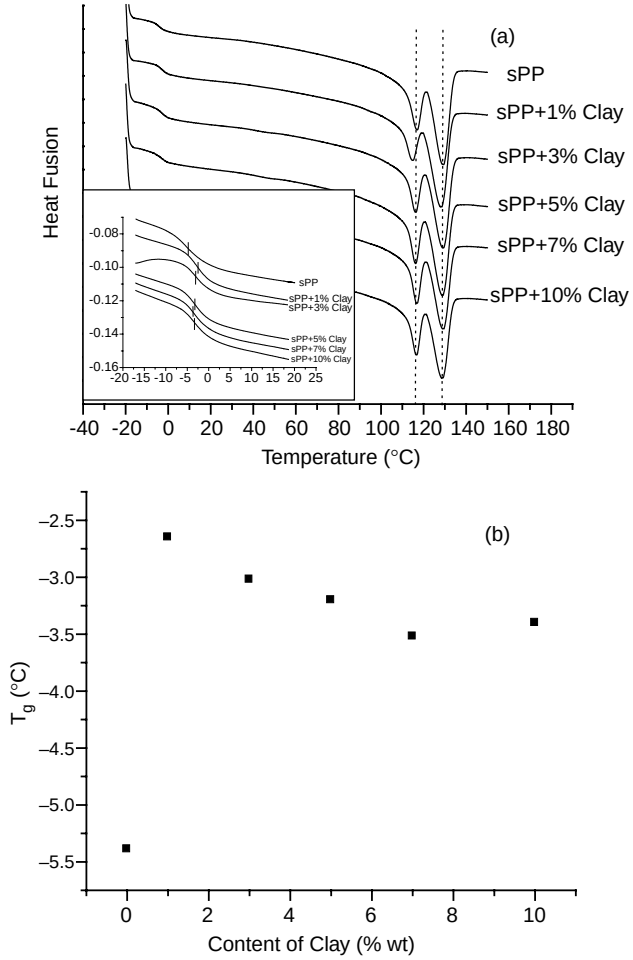

Fig. 8. (a) DSC thermographs for the sPP nanocomposites having different clay levels (b) change in the glass transition temperature (T_g) as a function of the content of the nanoclay.

helical form. In the temperature region between 60 and 90 °C a sharp increase in the ratio is observed, an indication that the transformation is mainly taking place in this region [43]. Comparing the thermal behavior of the samples, the sPP nanocomposites at 120 °C result in a situation where their polymeric chains contain again higher levels of helical conformation (the index varies from 1.4 to 1.48) respective to neat polymer (1.29).

Finally, differential scanning calorimetry (DSC) was used as an additional technique in order to study the thermal behavior of the nanocomposites. Fig. 8(a), which presents the DSC thermograms of sPP and sPP nanocomposites, depicts two endotherms characteristic of sPP. The lower temperature peak is attributed to the primary crystallites formed at corresponding T_c values, while the higher temperature peak to the recrystallizable crystallites formed during a subsequent heating scan after the melting of the secondary crystallites and the partial melting of the less stable fractions of the primary crystallites formed at the T_g [54], which can be related to the melting of the limit-disordered and the limit-ordered form I, respectively [54,55]. SPP nanocomposites show a slight decrease in the temperature [56] in both endothermic peaks respective to neat sPP. This decrease can be attributed to the smaller size of the crystallites in the polymeric matrix due the presence of the nanofiller, which interrupts the homogeneity of the polymer and constrain the crystallite development. It is obvious that the lower melting temperature is observed for low concentrations of clay. Furthermore, the DSC thermogramms show an increase in the glass transition temperature relative to the neat polymeric matrix, Fig. 8(b). It is well known that the glass transition temperature is associated with the mobility of the polymeric chains. As a consequence, the increase of the T_g can be attributed to the presence of the nanofiller in the sPP nanocomposites which means that the addition of the nanoclay constrains the motions of the chains. Finally, it can be seen in Fig. 8(b) that the glass transition temperature decreases slightly as the content of the nanofiller increases in agreement with a recent report in the literature [56].

4. Conclusions

The influence of the intercalation of a quaternary modified montmorillonite with syndiotactic polypropylene on the polymeric matrix's crystalline polymorphs was investigated using FT-IR and XRD spectroscopic techniques. Additionally, the effect of the presence of the nanoclay on the mechanical properties was investigated by means of dynamic mechanical analysis (DMA). FT-IR spectroscopy proved that the addition of the nanofiller affects the conformational structure ratio in the polymeric chains favoring the adoption of helical conformations. Furthermore, when tension is applied to the specimens that contain the nanofiller, the polymeric chains encounter a difficulty to achieve a high degree of transformation from the helical into the *trans*-planar form even at high elongations. Accordingly, when the applied tension is released, both the sPP nanocomposites and the neat sPP show a tendency to return to the initial helical conformation resulting in a citation where a combination of helical and *trans*-planar segments is finally present. However, in the case of the samples that contain the nanofiller, we find a higher proportion of chains characterized by helical conformation relative to the neat sPP in a similar situation. Furthermore, when highly stretched samples were exposed to heat the infrared analysis revealed that the polymeric chains contain higher levels of helical segments as well. In addition, infrared linear dichroism was used in order to study the orientation of the polymeric chains of sPP in the nanocomposites. It was found that the nanofiller constricts the orientation of the transition moment of the infrared bands that are attributed to the *trans*-planar conformation, whereas we find no clear influence on the orientation of an infrared band which is assigned to the helical conformation. XRD measurements showed that the melt-mixing of the organically modified silicates with sPP can result in intercalated structures when low concentrations of clay were used and partially intercalated structures for high nanofiller concentrations. Also, the application of mechanical stress to the nanocomposites can improve intercalation and partial exfoliation. Finally, dynamic mechanical analysis showed that the presence of the nanoclay results in a slight improvement of the mechanical properties of sPP, while via differential scanning calorimetry we found a small increase in the glass transition temperature of sPP, an implication that restriction in the movement of the polymeric chains takes place due to the presence of the nanoclay.

Acknowledgements

We thank Katherine A. Macchiarola of Panalytical Inc., Natick, MA, USA for acquiring the XRD patterns. This work was financially supported by the Greek Ministry of Development under the research grant PENED 2001-136.

References

[1] Usuki A, Kojima Y, Kawasumi M, Okada A, Fukusihima Y, Kurauchi TT, et al. J Mater Res 1993;8:1179.
[2] Kojima Y, Usuki A, Kawasumi M, Okada A, Kurauchi TT, Kamigaito O. J Polym Sci, Part A: Polym Chem 1993;31(4):983.
[3] Kawasumi M, Hasegawa N, Kato M, Usuki A, Okada A. Macromolecules 1997;30(20):6333.
[4] Manias E, Touny A, Wu L, Strawhecker K, Lu B, Chung TC. Chem Mater 2001;13(10):3516.
[5] Alexandre M, Dubois P, Sun T, Garces JM, Jérôme R. Polymer 2002;43: 2123.
[6] Tianxi L, Kian PL, Wuiwui CT, Pramoda KP, Zhi-Kuan C. Polymer 2003; 44:3529.
[7] Blumstein A. J Polym Sci, Part A: General Papers 1965;3(7):2665.
[8] Zhu J, Morgan AB, Lamelas FJ, Wilkie CA. Chem Mater 2001;13(10): 3774.
[9] Gilman JW, Jackson CL, Morgan AB, Harris Jr R, Manias E, Giannelis EP, et al. Chem Mater 2000;12(7):1866.
[10] Ray SS, Yamada K, Okamoto M, Fujimoto Y, Ogami A, Ueda K. Polymer 2003;44:6633.
[11] Ray SS, Okamoto M. Prog Polym Sci 2003;28:1539.
[12] Krishnamoorti RK, Vaia RA, Giannelis EP. Chem Mater 1996;8(8):1728.
[13] Giannelis EP. Adv Mater 1996;8(1):29.

[14] Ogata N, Jimenez G, Kawai H, Ogihara T. J Polym Sci, Part B: Polym Phys 1997;35:389.
[15] Wang Z, Pannavaia T. J Chem Mater 1998;10(7):1820.
[16] Vaia RA, Ishii H, Giannelis EP. Chem Mater 1993;5(12):1694.
[17] Heinemann J, Reichert P, Thomann R, Mülhaupt R. Macromol Rapid Commun 1999;20(8):423.
[18] Reichert P, Nitz H, Klinke S, Brandsch R, Thomann R, Mülhaupt R. Macromol Mater Eng 2000;275:8.
[19] Fornes TD, Yoon PJ, Keskkula H, Paul DR. Polymer 2001;42:9929.
[20] Ray SS, Maiti P, Okamoto M, Yamada K, Ueda K. Macromolecules 2002; 35(8):3104.
[21] Kaempfer D, Thomann R, Mülhaupt R. Polymer 2002;43:2909.
[22] Ewen JA, Jones RL, Razavi A, Ferrara JD. J Am Chem Soc 1988;110: 6255.
[23] Lotz B, Lovinger AJ, Cais RE. Macromolecules 1988;21(8):2375.
[24] Lovinger JA, Lotz B, Davis DD, Padden Jr FJ. Macromolecules 1993; 26(14):3494.
[25] De Rosa C, Corradini P. Macromolecules 1993;26(21):5711.
[26] Corradini P, Natta G, Ganis P, Temussi PA. J Polym Sci, Part C 1967;16: 2477.
[27] De Rosa C, Auriemma F, Corradini P. Macromolecules 1996;29(23): 7452.
[28] De Rosa C, Auriemma F, Vinti V. Macromolecules 1998;31(21):7430.
[29] Chatani Y, Maruyama H, Noguchi K, Asanuma T, Shiomura T. J Polym Sci, Part C: Polym Lett 1990;28:393.
[30] Natta G, Perlado M, Allegra G. Makromol Chem 1964;75:215.
[31] Natta G, Corradini P, Ganis P. Makromol Chem 1960;39:238.
[32] Nakaoki T, Ohira Y, Hayashi H, Horii F. Macromolecules 1998;31(8): 2705.
[33] Ohira Y, Horii F, Nakaoki T. Macromolecules 2000;33(5):1801.
[34] Nakaoki T, Yamanaka T, Ohira Y, Horii F. Macromolecules 2000;33(7): 2718.
[35] Vittoria V, Guadagno L, Comotti A, Simonutti R, Auriemma F, De Rosa C. Macromolecules 2000;33(16):6200.
[36] Chatani Y, Maruyama H, Asanuma T, Shiomura T. J Polym Sci, Part B: Polym Phys 1991;29:1649.
[37] Auriemma F, De Rosa C, Ruiz de Ballesteros O, Vinti V, Corradini P. J Polym Sci, Part B: Polym Phys 1998;36:395.
[38] Auriemma F, Ruiz de Ballesteros O, De Rosa C. Macromolecules 2001; 34(13):4485.
[39] De Rosa C, Gargiulo MC, Auriemma F, Ruiz de Ballesteros O, Razavi A. Macromolecules 2002;35(24):9083.
[40] Guadagno L, D'Aniello C, Naddeo C, Vittoria V. Macromolecules 2000; 33(16):6023.
[41] Guadagno L, D'Aniello C, Naddeo C, Vittoria V. Macromolecules 2001; 34(8):2512.
[42] Guadagno L, D'Aniello C, Naddeo C, Vittoria V, Meile SV. Macromolecules 2002;35(10):3921.
[43] Gatos KG, Kandilioti G, Galiotis C, Gregoriou VG. Polymer 2004;45: 4453.
[44] Bonnet M, Yan S, Petermann J, Zhang B, Yang D. J Mater Sci 2001;36: 635.
[45] Sozzani P, Simonutti R, Comotti A. Magnet Reson Chem 1994;32:s45.
[46] Asakura T, Aoki A, Date T, Demura M, Asanuma T. Polym J 1996;28:24.
[47] Ohira Y, Horii F, Nakaoki T. Macromolecules 2000;33(15):5566.
[48] Guadagno L, D'Aniello C, Naddeo C, Vittoria V, Meile SV. Macromolecules 2003;36(18):6756.
[49] Loos J, Hückert A, Petermann J. Colloid Polym Sci 1996;274:1006.
[50] Christy AA, Ozaki Y, Gregoriou VG. In: Barceló D, editor. Modern fourier: transform infrared spectroscopy in comprehensive analytical chemistry, vol. XXXV. Amsterdam, London, New York, Oxford, Paris, Shannon, Tokyo: Wilson and Wilson's, Elsevier; 2001.
[51] Gregoriou VG, Kandilioti G, Gatos KG. Vibr Spectrosc 2004;34:47.
[52] Lotz B, Mathieu C, Thierry A, Lovinger AJ, De Rosa C, Ruiz De Ballesteros O, et al. Macromolecules 1998;31(26):9253.
[53] Gorrasi G, Tortora M, Vittoria V, Kaempfer D, Mülhaupt R. Polymer 2003;44:3679.
[54] Supaphol P. J Appl Polym Sci 2001;82:1083.
[55] Aurimma F, De Rosa C, Corradini P. Macromolecules 1993;26(21):5719.
[56] Tu-Qing Z, Joong-Hee L, Rhee MJ, Rhee YK. Comp Sci Technol 2004; 64:1383.